Available online at www.sciencedirect.com
ScienceDirect
Journal of Catalysis 246 (2007) 399–412
JOURNAL OF CATALYSIS
www.elsevier.com/locate/jcat

# Marked influence of support on the catalytic performance of PdSb acetoxylation catalysts: Effects of Pd particle size, valence states, and acidity characteristics ☆

V. Narayana Kalevaru [a], A. Benhmid [b], J. Radnik [a], M.-M. Pohl [a], U. Bentrup [a], A. Martin [a,*]

[a] *Leibniz-Institute for Catalysis (former ACA), Richard-Willstätter-Str. 12, D-12489 Berlin, Germany*
[b] *Chemistry Department, Garyounis University, Benghazi, P.O. Box 1308, Libya*

Received 10 November 2006; revised 5 January 2007; accepted 5 January 2007

Available online 6 February 2007

**Abstract**

The influence of support on the catalytic performance of PdSb catalysts for the gas-phase acetoxylation of toluene was investigated using various support materials with different acid strengths and surface areas. The supports used were $TiO_2$, $ZrO_2$, $SiO_2$, and $\gamma$-$Al_2O_3$. The catalysts were characterized by $N_2$ adsorption (BET-SA and pore size distribution), XRD, TEM, XPS, and FTIR (pyridine adsorption), and their performance in the selective acetoxylation of toluene to benzyl acetate (BA) was evaluated. Electron micrographs of spent solids exhibited considerably larger Pd particles compared with the corresponding fresh solids, indicating growth of Pd particles during the course of reaction, depending on the support. Such Pd growth was accompanied by enhanced catalytic performance. XPS revealed that the nature of support had a clear influence on the reducibility of Pd. The samples prepared with reducible supports (i.e., $TiO_2$, $ZrO_2$) displayed a substantial decrease in surface Sb and Pd/metal ratios in the used samples compared with fresh samples. In contrast, no such changes occurred with nonreducible supports ($SiO_2$ and $\gamma$-$Al_2O_3$). Acidity measurements by means of pyridine adsorption disclose that all of the PdSb samples, irrespective of support-exhibited bands, correspond solely to Lewis sites; no evidence of Brønsted sites was found. The present study was aimed at determining the acidic strength of the catalysts based on catalytic performance. Changes in catalytic activity with time on stream were found to be dependent on the type of support used. Achieving steady-state conditions took longer in $TiO_2$-supported catalyst (ca. 10 h) than with other supports (ca. 3 h). The best results were obtained over a 10Pd8Sb/$TiO_2$ catalyst (10 wt% Pd, 8 wt% Sb; $X_{TOL} = 68\%$, $S_{BA} = 85\%$) compared with all other catalysts of this series. Evaluating the nature of the supports revealed very pronounced differences in terms of Pd particle size, valence states, and acidity characteristics, which in turn showed a significant effect on the catalytic performance. However, growth of Pd particles and higher Lewis acidity represent a major requisite for obtaining better catalytic performance.


*Keywords:* Influence of support; Gas phase acetoxylation; Pyridine adsorption (FTIR); XRD; TEM; XPS; Effects of Pd particle size; Valence states; Acidity characteristics

## 1. Introduction

Supported metal or metal oxide catalysis has been the subject of extensive research from both academic and industrial standpoints because of the wide spread use of supported catalysts for different catalytic applications [1–3]. The performance of supported metal catalysts is generally governed by a complex mix of different contributions arising from metal particle size, shape, morphology, metal dispersion, electronic state, and other features. Numerous articles [4–7] have indicated that the nature of a support can have a significant effect on the activity and selectivity behavior of the catalysts. A literature survey [8,9] reveals that the acidic supports normally enhance the electron deficiency on the noble metal more than the basic ones do. Other factors that must also be considered along with the support include the extent of metal loading, catalyst preparation, pretreatment conditions, Pd particle size, the nature of the sup-

☆ Dedicated to Professor Dr. Bernhard Lücke on the occasion of his 70th birthday.

* Corresponding author. Fax: +49 30 6392 4454.
*E-mail address:* andreas.martin@catalysis.de (A. Martin).

0021-9517/$ – see front matter 
doi:10.1016/j.jcat.2007.01.002

port, and the presence of additional co-components (e.g., transition metals) [10]. Supported Pd catalysts in particular have found widespread application in industrial reactions [11–13]. Interestingly, Pd-based catalysts are also widely used for acetoxylation reactions.

Acetoxylation of olefins and/or aromatic hydrocarbons is not only a special type of partial oxidation for direct synthesis of industrially important esters, but also a simple, effective, and straightforward method for such processing. A representative example is the gas-phase oxidation (acetoxylation) of toluene, in which toluene, acetic acid, and oxygen are catalyzed by suitable Pd-based catalysts to produce benzyl acetate (BA) in a single step. Acetoxylation of toluene in particular is of great industrial importance, because the target product (BA) is widely used in the perfume, food, and chemical industries. Although many synthetic investigations (mostly liquid phase) have appeared in the literature on the acetoxylation of toluene, these studies are associated with various problems. Studies on the gas-phase processes are scarce. Thus, the development of an efficient vapor-phase process for the direct synthesis of esters in general, and BA in particular, has recently become of interest.

The first of our earlier studies was devoted to PdSb/$TiO_2$ system over a wide range of palladium loadings [14] and achieved an excellent performance compared with existing literature reports [15,16]. The 20Pd8Sb/$TiO_2$ (20 wt% Pd, 8 wt% Sb) catalyst gave a high conversion of toluene ($X \geqslant 90\%$) with high selectivity of BA ($S = 85\%$). Although these catalysts exhibited amazingly high conversions and selectivities, they underwent deactivation with time-on-stream. In subsequent efforts to overcome such deactivation problems, these catalysts were further modified using different promoters [17], which successfully improved catalyst lifetime and BA selectivity (up to 95%) [18]. In addition, intense investigations were also carried out in such areas as optimization of reaction conditions [19], influence of Pd loading [20], influence of Sb loading [21], and enhancement of catalyst lifetime and investigation of the catalyst deactivation phenomenon [22].

Up to now, the size of Pd particles has been assumed to have a clearly dominant influence on catalytic performance. However, acidity of the catalysts also appears to be an important factor in influencing catalytic performance. Thus, estimating the nature, amount, and strength of acidic sites is essential to deriving acidity–activity relationships. Various techniques have been applied, and many articles on determining the acidity of different solids have been published [23–26]. Among the various techniques suggested for acidity measurements, FTIR spectroscopy is one of the most widely accepted and used. The benefit of this technique is its ability to readily distinguish Lewis acid sites from Brønsted acid sites. In view of this, in the present study we also applied FTIR spectroscopy (using pyridine as a basic probe) to estimate the number of acid sites and verify their influence on catalytic properties.

The primary objective of the present investigation is to evaluate the influence of various oxide supports (i.e., $TiO_2$, $SiO_2$, $\gamma$-$Al_2O_3$, and $ZrO_2$) on the activity and selectivity behavior of PdSb-containing solids. Another aim is to summarize our understanding of the potential effects induced by different supports, particularly on Pd particle size, valence states, and acidity characteristics, and their influence on catalytic performance.

## 2. Experimental

### 2.1. Catalyst preparation

Catalysts were prepared by impregnation using a two-step method. Step 1 involved impregnation of an aqueous solution of $SbCl_3$ (Alfa Produkte, Karlsruhe, Germany) onto the support using a constant amount of Sb (8 wt%) with respect to the total amount of the catalyst. The solid mass was then dried in an oven at 120 °C for 16 h, followed by calcination at 400 °C for 3 h in air (50 ml/min).

In step 2, the aforementioned Sb-impregnated sample was further impregnated with an appropriate amount of acidified aqueous solution of $PdCl_2$ (99.8%, Alfa Produkte, Karlsruhe, Germany) to get the desired amount of Pd (10 wt%). The excess solvent was removed by rota vapor, and the sample was dried in an oven at 120 °C for 16 h. Then in situ activation of the samples was performed one after the other at 300 °C for 2 h in air in the catalytic reactor before activity testing and characterization.

Such oxidative treatment permits the removal of chlorides from the catalyst precursors and facilitates their transformation into Pd and PdO phases, the concentrations of which, however, depend on the nature of support used. Therefore, note that hereinafter "fresh" catalyst means always in situ activated catalyst (300 °C for 2 h in air). In a similar fashion, all of the catalysts were prepared using four different oxide supports such as $TiO_2$, $ZrO_2$, $SiO_2$, and $\gamma$-$Al_2O_3$. More details on catalyst preparation have been reported elsewhere [27,28]. The denotation and composition of different samples prepared are presented in Table 1. The composition of the materials was checked by inductively coupled plasma optical emission spectrometry (ICP-OES), and the values were found to be close to the theoretical ones.

In addition, four more samples (in the absence of Pd), including 8Sb/$TiO_2$, 8Sb/$ZrO_2$, 8Sb/$SiO_2$, 8Sb/$\gamma$-$Al_2O_3$ (8 wt% Sb each), were prepared in a similar way as described in step 1. The intent was to characterize these four catalysts by FTIR (pyridine adsorption) and compare their acidity parameters in the presence and absence of Pd in these solids.

### 2.2. Characterization of catalysts

The BET surface areas and pore size distribution of the catalysts were determined using a Micromeritics Gemini III 2375 instrument by $N_2$ physisorption at −196 °C. Before the measurements, the known amount of catalyst was evacuated for 2 h at 150 °C to remove physically adsorbed water.

X-ray diffraction (XRD) patterns were obtained using a STADI-P X-ray diffractometer (Stoe, Germany) with Ni-filtered Cu$K_\alpha$ radiation ($\lambda = 154.18$ pm). The samples were analyzed after deposition on a Stoe quartz monocrystal sample holder. The crystalline phases were identified by referring to the ASTM data files.

Samples for transmission electron microscopy (TEM) were prepared by depositing the sample on a copper grid (300 mesh)

Table 1
The denotation, composition, BET surface areas, and pore volumes of PdSb catalysts with different supports

| Denotation | Catalyst composition | Fresh (activated) BET-SA ($m^2/g$) | Catalysts pore volume ($cm^3/g$) |
|---|---|---|---|
| 10Pd8Sb/$TiO_2$ | 10 wt% Pd, 8 wt% Sb/$TiO_2$ | 78.1 | 0.128 |
| 10Pd8Sb/$ZrO_2$ | 10 wt% Pd, 8 wt% Sb/$ZrO_2$ | 46.6 | 0.108 |
| 10Pd8Sb/$SiO_2$ | 10 wt% Pd, 8 wt% Sb/$SiO_2$ | 192.6 | 0.542 |
| 10Pd8Sb/$\gamma$-$Al_2O_3$ | 10 wt% Pd, 8 wt% Sb/$\gamma$-$Al_2O_3$ | 98.8 | 0.211 |
| – | Pure $TiO_2$[a] | 315 | 0.273 |
| – | Pure $ZrO_2$ | 206 | 0.225 |
| – | Pure $SiO_2$ | 392 | 0.573 |
| – | Pure $\gamma$-$Al_2O_3$ | 249 | 0.471 |

[a] Uncalcined sample.

coated with lacy carbon film. TEM analysis was performed using a CM-20 microscope (twin) (Philips, The Netherlands) at 200 kV with EDAX PV9900.

The X-ray photoelectron spectroscopic (XPS) measurements were done with an ESCALAB 220iXL (VG Instruments, UK). Al$K_\alpha$ radiation was used to obtain the XP spectra. The spectra were referred to the main peak of cationic components of the support (Ti $2p_{3/2}$ of $TiO_2$ at 458.8 eV, Zr $3d_{5/2}$ of $ZrO_2$ at 182.2 eV, Si 2p of $SiO_2$ at 103.3 eV, and Al 2p of $Al_2O_3$ at 74.4 eV). The binding energy (BE) scale was calibrated with pure, clean Cu, Ag, and Au samples. For quantitative analysis after Shirley background subtraction, the peaks were fitted with Gaussian–Lorentz curves. The peak areas thus obtained were divided by the element-specific Scofield factor and the analyser-specific transmission function to get the composition in the near-surface region.

For the characterization of surface acidity, pyridine was adsorbed on the activated catalysts at room temperature until saturation. Before the adsorption experiments, the catalysts were again activated by heating in airflow at 300 °C for 30 min. Spectra were recorded using a Bruker IFS 66 spectrometer (2 $cm^{-1}$ resolution, 100 scans) equipped with a heatable and evacuable IR cell with $CaF_2$ windows connected to a gas dosing/evacuation system. For these experiments, the catalyst powder was pressed into self-supporting discs (50 mg, $\phi = 20$ mm). Difference spectra were obtained by subtracting the spectrum of the activated catalyst at room temperature.

### 2.3. Activity measurements

Acetoxylation runs were performed in a fixed-bed, on-line micro-catalytic reactor. About 1 ml of catalyst particles (size, 0.425–0.6 mm) was loaded into the stainless steel reactor. The reaction was performed at 210 °C and 2 bar. Argon (99.99%), used as a dilution gas, and synthetic air, used as a source of oxygen, were supplied from commercially available compressed gas cylinders and used without further purification. The catalyst was activated in airflow (27 ml/min) at 300 °C for 2 h before the activity measurements. The organic feed mixture (i.e., toluene + acetic acid mixture prepared in the mole ratio of 1:4) was pumped to the reactor using HPLC pump.

All of the catalytic tests were performed under identical conditions as follows: the molar ratio of toluene:acetic acid:oxygen (air):argon = 1:4:3(15):16, $T = 210$ °C, GHSV (STP) = 2688 $h^{-1}$, $\tau = 1.34$ s. The product stream was analyzed on-line by gas chromatography (HP-5890) using an HP-5 capillary column (50 m × 0.32 mm) and a flame ionization detector. The column outlet was connected to a methanizer (30% Ni/$SiO_2$ catalyst), which converted all of the carbon-containing products, including CO and $CO_2$, into methane. This allowed the reliable and simple quantitative analysis of the products with the flame ionization detector module. More details on the experiment and product analysis have been given elsewhere [20].

## 3. Results and discussion

### 3.1. BET surface areas and pore size distribution

BET surface areas and pore volumes of the fresh (activated) catalysts prepared with four different supports are presented in Table 1. Of the four supports used, the surface area of the $TiO_2$ (anatase)-supported catalyst decreased drastically (from 315 to 78 $m^2/g$) after impregnation of both Sb (8 wt%) and Pd (10 wt%). This is because the anatase sample used for this preparation was an uncalcined sample (i.e., anatase precursor), unlike other supports. However, no such drastic decrease in surface area was seen in the catalysts prepared with other supports. These decreases in surface area and pore volume after the deposition of Sb and Pd is due mainly to penetration of dispersed Pd and Sb species into the pores of the support, as well as to solid-state reactions between the dispersed components and the support. But the extent of decrease in surface areas depends on the nature of the support applied. Table 1 shows that of all of the supports studied in this series, $SiO_2$-supported Pd catalyst exhibited the highest surface area (193 $m^2/g$) and pore volume (0.542 $cm^3/g$); $ZrO_2$ had the lowest surface area (47 $m^2/g$) and pore volume (0.107 $cm^3/g$).

Pore size distributions of fresh (activated) and used catalysts are portrayed in Figs. 1a and 1b. These figures clearly show that all of the fresh and used catalysts exhibited unimodal pore volume distribution. Although all of these catalysts had a unimodal distribution, they had some differences, especially in terms of pore size and distribution (Figs. 1a and 1b). Such differences in pore size are due to differences in the type of oxide supports applied and their varying surface areas. The catalysts prepared with reducible supports ($TiO_2$, $ZrO_2$) with low surface areas

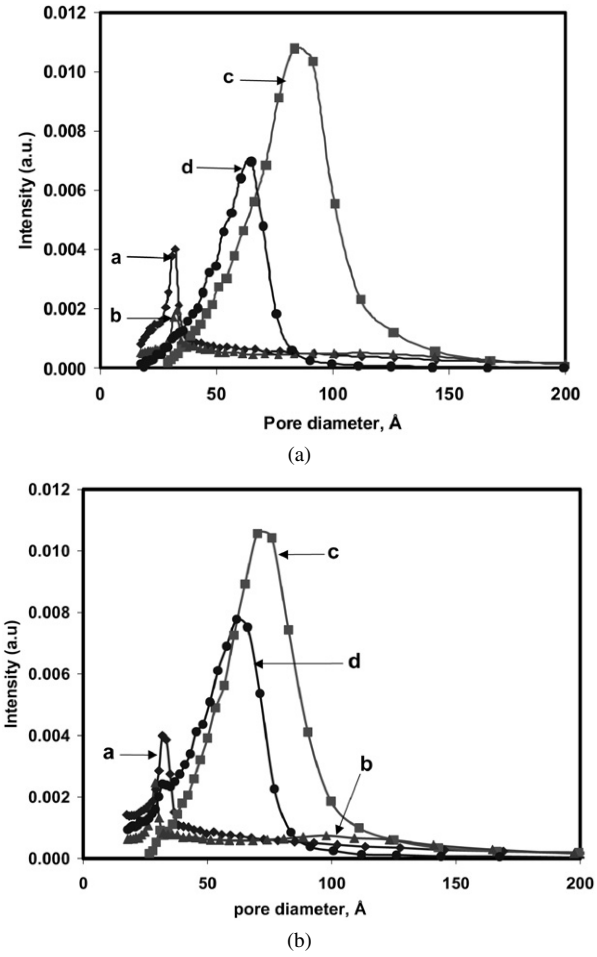


Fig. 1. Pore volume distribution of the (a) fresh and (b) 10Pd8Sb catalysts with different supports (a: $TiO_2$; b: $ZrO_2$; c: $SiO_2$; d: $\gamma$-$Al_2O_3$).

showed a narrow distribution in the range of ca. 20–50 Å with a dominant pore diameter around 35 Å. On the other hand, the catalysts with high surface areas ($SiO_2$, $\gamma$-$Al_2O_3$) displayed a considerably broader range of pore size distribution, from ca. 25–150 Å, with dominant pore diameters around 85 Å ($SiO_2$) and 60 Å ($\gamma$-$Al_2O_3$), respectively. Careful examination of the pore volume distributions of the fresh and used catalysts shows a trend toward a lower pore size range (i.e., 25 to ca. 120 Å), particularly for the $SiO_2$-supported used catalyst. Pores larger than 100 Å are largely absent in this particular spent catalyst, probably due to an increase in the size of Pd as a result of sintering during the reaction. Such sintering of Pd is also well evidenced on XRD; both the $SiO_2$ and $\gamma$-$Al_2O_3$ fresh samples were X-ray amorphous, whereas the used samples became more crystalline.

### 3.2. XRD

XRD patterns of the fresh (activated) and spent catalysts are shown in Figs. 2a and 2b. Of the four different supports investigated, a reflection corresponding to the Pd phase besides the typical anatase reflections can be seen only in the (fresh) $TiO_2$-supported catalyst. In the $ZrO_2$-supported catalyst, a reflection belonging to the PdO phase can be seen.

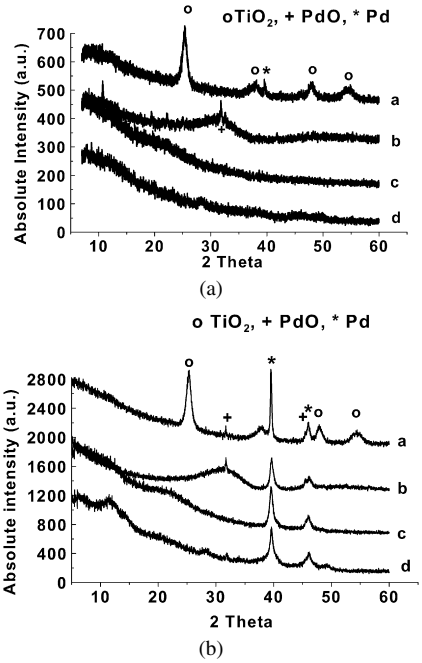


Fig. 2. XRD patterns of the (a) fresh and (b) 10Pd8Sb catalysts with different supports (a: $TiO_2$; b: $ZrO_2$; c: $SiO_2$; d: $\gamma$-$Al_2O_3$).

In addition, in the $ZrO_2$-supported Pd catalyst, a new reflection at $2\theta = 10.7°$ (Figs. 2a and 2b) appeared, probably due to the formation of a new phase. This new reflection appeared in the fresh catalyst but disappeared in the used catalyst. $SiO_2$- and $\gamma$-$Al_2O_3$-supported PdSb (fresh) catalysts are found to be X-ray amorphous. Note that the crystallinity of all of the used samples increased during the course of reaction under the influence of the reaction conditions. Among the four supports investigated, the crystallinity of titania (anatase) was dramatically increased in the used catalyst, as evidenced by the intense reflections belonging to the $TiO_2$ phase. This finding is well supported by the TEM analysis, which showed a nearly fourfold increase in the size of support $TiO_2$ particles (ca. 25 nm) compared with the fresh sample (ca. 6 nm). All of the used Pd catalysts showed the reflections corresponding to two types of palladium phases, such as oxidized palladium (PdO) and metallic palladium (Pd), irrespective of the type of support used. Interestingly, the intensity of reflections belonging to these two phases was higher in the used reducible supports ($TiO_2$ and $ZrO_2$) than in the nonreducible supports ($SiO_2$ and $\gamma$-$Al_2O_3$).

Furthermore, in the used catalysts the major intense reflection corresponds to metallic Pd(111) at $2\theta = 40°$ is marginally shifted to lower angles. This marginal shift in the value of $2\theta$ might be due to a possible formation of some traces of carbide-phase ($PdC_x$) [29]. However, we did not observe any such crystalline palladium carbide phase from our XRD analysis. According to Krishnankutty et al. [30,31] the carbon dissolves in the Pd lattice, as the larger Pd particles are captious sink for the carbon. In the present study, the carbon contents in the used catalysts were estimated to be ca. 5 wt%; therefore, the formation of such amorphous $PdC_x$ phase in smaller amounts may not be excluded.

### 3.3. Transmission electron microscopy (TEM)

Electron micrographs of the fresh (activated) and used PdSb samples with different supports are depicted in Figs. 3a and 3b. All of these catalysts showed a narrow size particle distribution of Pd, but with varying sizes, depend on the type of support used. An interesting finding is that $TiO_2$- and $SiO_2$-supported samples displayed significant Pd growth, whereas $ZrO_2$ contained a mixture of smaller and larger Pd particles, and $\gamma$-$Al_2O_3$ showed no considerable growth of Pd during the reaction. As a result of such deviations, catalytic performance also changes in accordance with the Pd particle size. It can be seen from Fig. 3a (a) that the fresh $TiO_2$-supported catalyst exhibited relatively larger Pd particles compared with the other supports. The Pd particles on $TiO_2$ support were spherical shaped and ranged in size from 1 to 10 nm. Shen et al. [32] reported from their TEM analysis on $TiO_2$-supported Pd catalysts with different Pd loadings that Pd particles are hemispherical in shape with a narrow size distribution of 4–20 nm, which are fixed in the well developed planes of $TiO_2$. As a result of such matching, these authors suggested that the support structure could stabilize Pd particles and favor strong metal–support interaction. In the case of fresh $SiO_2$-supported catalyst (Fig. 3a (c)), the Pd particles are uniformly distributed on the support with size ranging from 2 to 4 nm and shape again nearly spherical. These results are in agreement with those reported by Kochubey et al. [33]. $ZrO_2$- and $\gamma$-$Al_2O_3$-supported catalysts (Fig. 3a (b and d)) showed Pd morphology similar to that of $TiO_2$- and $SiO_2$-supported ones but with smaller Pd particles. Among the four fresh solids investigated, the $ZrO_2$-supported catalyst (Fig. 3a (b)) exhibited very small Pd particles (1.5–2 nm) with a narrow size distribution, more or less comparable to the $\gamma$-$Al_2O_3$-supported solid. The decreasing order of Pd particle size in these fresh PdSb catalysts over the different supports is as follows:

$$TiO_2 > SiO_2 > ZrO_2 \sim Al_2O_3. \quad \text{(i)}$$

Although this order is not changed in the used catalysts, there is a dramatic increase in the size of Pd particles in the spent materials compared with their corresponding fresh ones (Fig. 3b). The size of Pd particles in the used $TiO_2$-supported catalyst (Fig. 3b (a)) was increased even up to 100 nm due to agglomeration. Even though the small Pd particles that were seen in this fresh catalyst almost disappeared, most of the particles still retained their morphology (i.e., hemispherical shape), similar to fresh catalyst. A similar increase in the size of Pd particles in the used samples was also noted by Lyubovsky et al. [34], who reported that most of the Pd particles were round and some were as large as 200–300 nm. This growth in particle size in the used samples is attributed to the restructuring of metal particles during the course of reaction.

In the $SiO_2$-supported sample (Fig. 3b (c)), some of the Pd particles grew to between 10 and 60 nm, and in a few instances, formation of certain single particles up to 200 nm was observed. In other words, this catalyst contains mixture of Pd particles with varying sizes, ranging from small (ca. 10 nm) to large (ca. 60 nm), with a few very large particles (ca. 200 nm). In some of the largest particles, there is indication of the formation of an intermetallic phase between Pd and Sb. In addition, the image of this sample, shown in Fig. 3b (c*)), reveals an interesting result on the covering of Pd particles by carbon layers: an estimated ca. 7-nm-thick carbon layer covered this particular Pd particle.

The changes in the Pd particle size of $ZrO_2$ and $\gamma$-$Al_2O_3$ used samples were somewhat different, as was their catalytic behavior. For instance, $ZrO_2$-supported catalyst (Fig. 3b (b)) exhibited certain growth in the size of Pd particles and also contained mixtures of Pd particles ranging in size from 10 to

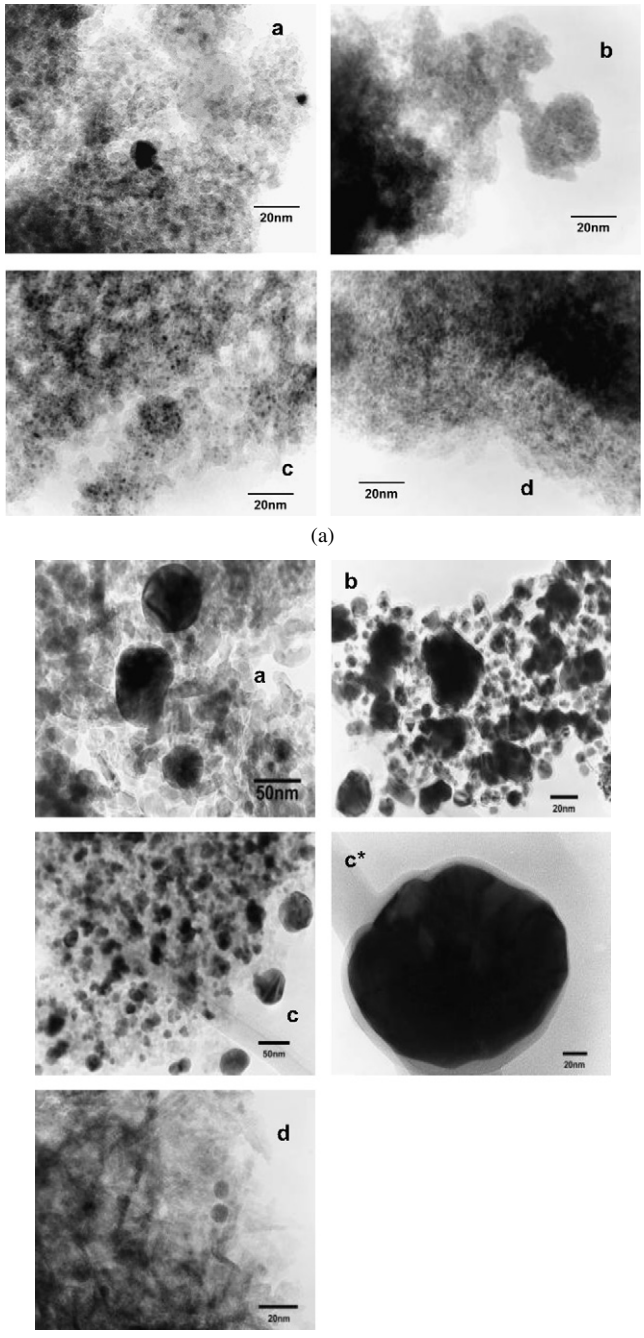


Fig. 3. Electron micrographs of the (a) fresh and (b) 10Pd8Sb catalysts with different supports (a: $TiO_2$; b: $ZrO_2$; c: $SiO_2$; d: $\gamma$-$Al_2O_3$; c*: big Pd particle covered with carbon layer).

(a few) ca. 90 nm. In other words, this sample contained more smaller particles than larger ones. It is noteworthy that this catalyst also sometimes exhibited the deposition of carbon layers of considerable thickness (ca. 5–7 nm) on the surface of the Pd particles, similar to what was seen in the $SiO_2$-supported sample. Surprisingly, in contrast to the above observations, the $\gamma$-$Al_2O_3$-supported sample (Fig. 3b (d)) exhibited significant resistance toward the growth of Pd particles during the course of the reaction, and hence its spent sample contained significantly smaller Pd particles than the others. The size of Pd particles in the $\gamma$-$Al_2O_3$-supported used sample varied over only a small range (5–10 nm), much less that that of the $TiO_2$-supported sample in particular and the other solids in general. Differences in the relative resistance to the growth of Pd particles (metal sintering) caused by the use of dissimilar supports can also be ascribed to the differences in the degree of interaction between metal particles and the carrier surface.

In contrast to the morphology and size of Pd particles, it was quite surprising to note that no free Sb particles with distinct morphology were detected in any of these solids despite their high Sb content (8 wt%). In the same way, no free Sb particles were seen even in the pure Sb/$TiO_2$ sample (in the absence of Pd) and in the samples with very high Sb contents (e.g., 20Sb10Pd/$TiO_2$) [21]. In a similar way, XPS analysis was also not really very useful in gaining deeper insights, particularly on Sb species. However, the presence of Sb had a beneficial role on catalytic performance. Earlier investigations [21] focusing on the effect of Sb on Pd particle size as well as catalytic performance confirmed that the absence of Sb inhibits the growth of Pd particles and drastically reduces the catalytic activity. Furthermore, such a situation (i.e., use of non-Sb-containing Pd catalysts) also diverts the reaction in undesired direction, giving only total oxidation products (i.e., $CO_x$) instead of the desired product, benzyl acetate [20]. Thus, it can be understood that one of the main roles of Sb is to influence the growth mechanism of Pd particles and thereby enhance the catalytic performance. It was also interesting to note from previous work [21] that the size of Pd particles in monometallic 10Pd/$TiO_2$ (in the absence of Sb) with a similar Pd content as in the present study, was very small and even difficult to measure due to weak contrast. This result implies that the presence of certain amount of Sb is needed for obtaining larger Pd particles that are needed for better acetoxylation activity. Nevertheless, the TEM investigations provided no further insight into the role of Sb as a co-component of this system. Only the $SiO_2$-supported catalyst showed some hints of the formation of an intermetallic phase between Pd and Sb in the particles larger than 200 nm. However, no indication for such a phase formation was found over any of the other supported samples except $SiO_2$. This result also agreed with the X-ray diffractograms showing no known PdSb phase. In all of these samples, independent of reaction time, no free Sb particles were detected, and the Sb was always observed to be together with the support. Thus, major changes were found only in the size of Pd particles.

Summing up, it is conceivable that the support has a strong influence on the growth of Pd particles during the course of the reaction. The changes in Pd particle size in these catalysts also has a significant influence on the catalytic performance of the catalysts.

### 3.4. XPS

In accordance with TEM investigations, XPS measurements also confirmed the strong influence of the nature of the support on the catalytic properties of the Pd particles. Fig. 4 compares the XP spectra of fresh and used PdSb samples with different supports. Note that for the $ZrO_2$-supported palladium catalyst, an overlap can be observed between Zr $3p_{3/2}$ ($BE = 332.6$ eV) and Pd $3d_{5/2}$ ($BE = 335.2$ eV) states, due to their close BE values. XPS revealed that all of the fresh catalysts except the $SiO_2$-supported one exhibited exclusively oxidized surface Pd species with BE values of 337.6 eV. The $SiO_2$ supported solid showed both oxidized and metallic Pd species (Fig. 4). Spent catalysts also showed some differences in surface composition compared with the fresh samples. Used $TiO_2$- and $\gamma$-$Al_2O_3$-supported solids exhibited both metallic and oxidized Pd species, indicating a certain degree of reduction in these samples. On the other hand, $ZrO_2$- and $SiO_2$-containing solids showed exclusively metallic Pd species, revealing a complete reduction of oxidized Pd species during the course of the reaction.

Another notable difference is that the surface composition of these catalysts differs from that of bulk composition. This aspect can be readily seen when comparing XPS and XRD results (see Figs. 2 and 4). The phase compositions in the surface (XPS) and the bulk (XRD) in both the fresh and used samples are given in Table 2. As mentioned earlier, all of the fresh samples (except the $SiO_2$-supported one) contained 100% oxidized palladium species at the surface (XPS), as expected due to the oxidation pretreatment (300 °C for 2 h in air) given to the catalysts before catalytic runs. Only the $SiO_2$-supported fresh sample contained both oxidized Pd and metallic Pd at its surface. Careful analysis of bulk composition (analyzed by XRD) shows that $TiO_2$-supported sample contained metallic Pd in contrast to XPS, whereas the $ZrO_2$-supported one exhibited a PdO phase

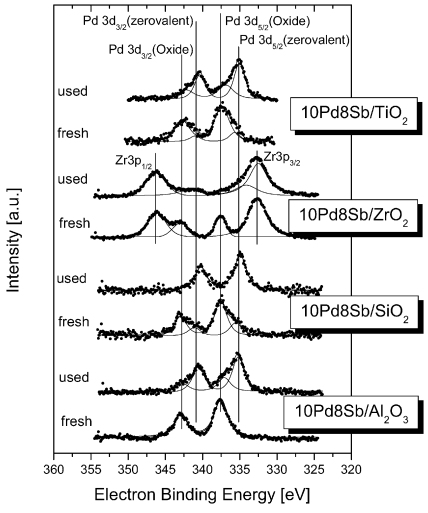


Fig. 4. Normalized XP spectra of the Pd 3d state after Shirley background subtraction of the fresh and used PdSb/Me catalysts with different supports (Me = $TiO_2$, $SiO_2$, $Al_2O_3$, $ZrO_2$).

Table 2
Comparison of phase composition between surface (XPS) and bulk (XRD) of 10Pd8Sb samples with different supports

| Catalyst | XPS (surface) | | XRD (bulk) | |
|---|---|---|---|---|
| | Fresh | Used | Fresh | Used |
| 10Pd8Sb/$TiO_2$ | 100% PdO | 65% Pd, 35% PdO | Pd | Pd, PdO |
| 10Pd8Sb/$ZrO_2$ | 100% PdO | 100% Pd | PdO | Pd, PdO |
| 10Pd8Sb/$SiO_2$ | 71% PdO, 29% Pd | 100% Pd | X-ray amorphous | Pd, PdO[a] |
| 10Pd8Sb/$\gamma$-$Al_2O_3$ | 100% PdO | 74% Pd, 26% PdO | X-ray amorphous | Pd, PdO[a] |

[a] Weak reflections.

similar to that seen on XPS (surface) analysis. The other two fresh samples ($SiO_2$ and $\gamma$-$Al_2O_3$) are X-ray amorphous. Such differences between the surface and bulk can be assumed from the differences in the particle sizes and surface effects; that is, smaller particles typical of the $ZrO_2$ support and Pd atoms at the surface seem to be rather oxidized, whereas larger ones on $TiO_2$ have a metallic Pd core. The mild oxidative activation treatment that the catalysts underwent before catalytic runs might also be another reason for such deviations. This mild activation treatment at low temperature (300 °C for 2 h in air) seems not strong or severe enough to oxidize the entire Pd present in its bulk and is able to oxidize Pd species only in the near-surface region, which can easily be estimated by XPS. It is known that XRD as a bulk method is more sensitive for larger crystalline particles.

Moreover, the phase composition at the surface (XPS analysis) is also found to be different from bulk (XRD analysis) even in the used samples. All four used samples characterized by XRD (bulk) showed both oxidized and metallic Pd in different proportions. The intensities of the reflections suggest that the amount of Pd seems to be higher on the reducible supports than on the irreducible supports. Another possible explanation for these intensities could be the lower crystallinity of the oxidized species, which could mean that the PdO particles are smaller. However, XPS showed that only the $TiO_2$- and $\gamma$-$Al_2O_3$-supported samples exhibited both metallic and oxidized Pd, whereas the other two samples contained only metallic Pd species. Comparing these results with the TEM observations on Pd particle growth during time on stream does not allow a simple correlation between Pd particle size and valence states. $TiO_2$-supported catalyst with larger Pd particles have the same Pd valence states in the near-surface region as the $Al_2O_3$-supported sample with smaller Pd particles. In addition, no correlation between the reducibility and the valence states can be established. These results undoubtedly suggest that the nature of support has a clear influence on the reducibility of Pd and hence the valence states of Pd. Nevertheless, it remains unclear exactly how the support influences these properties. Our results do provide some insight into the nature of support influencing the phase composition of the catalysts between the surface and the bulk, however.

Careful observation of the surface oxidized and reduced Pd species given in Table 2 reveals that the concentration and the distribution of these two Pd species depend on the type of support applied. Characterization of spent catalysts showed that the reaction conditions and feed composition brought about considerable changes in the distribution of these two different surface Pd species. Spent $ZrO_2$- and $SiO_2$-supported samples exhibited 100% metallic Pd species, whereas $TiO_2$ and $\gamma$-$Al_2O_3$ samples had both oxidized and metallic Pd species in different proportions (Table 2). Comparing fresh and used zirconia-supported PdSb catalyst shows that the fresh catalyst contained exclusively oxidized Pd (i.e., $PdO_x$), whereas the used sample (after 10 h on stream) contained exclusively metallic Pd species, indicating a complete reduction of oxidized species during the course of the reaction. This result points to the fact that this support facilitates easy reduction and oxidation of palladium species. On the other hand, the $SiO_2$-supported fresh sample contained a mixture of $PdO_x$ (71%) and metallic Pd (29%) species, whereas the used sample showed only reduced Pd species (i.e., 100%, after 16 h on stream). It appears that the Pd species over this catalyst are easily reducible but not easily oxidizable. These results undoubtedly suggest that the nature of the support has a clear influence on the reducibility of Pd and hence the valence states of Pd. Moreover, it is somewhat difficult at this stage to assess the extent of degree of reduction of Pd that is critical to obtaining better catalyst performance. Further studies are needed to estimate the suitable amounts of reduced and oxidized surface Pd species that are essential for controlling the activity and selectivity behavior of the catalysts.

Table 3
Changes in the Pd/Me and Sb/Me ratios, in the near-surface region between fresh and used catalysts (Me = Ti, Zr, Si, Al)

| Catalyst | Pd/Me | | Sb/Me | |
|---|---|---|---|---|
| | Fresh | Used | Fresh | Used |
| 10Pd8Sb/$TiO_2$ | 0.10 | 0.08 | 0.12 | 0.08 |
| 10Pd8Sb/$ZrO_2$ | 0.15 | 0.12 | 0.14 | 0.10 |
| 10Pd8Sb/$SiO_2$ | 0.03 | 0.03 | 0.01 | 0.02 |
| 10Pd8Sb/$\gamma$-$Al_2O_3$ | 0.06 | 0.06 | 0.04 | 0.03 |

Table 3 compares Pd and metal (Pd/Me) and of Sb and metal (Sb/Me) near-surface ratios in the fresh and used PdSb catalysts with different supports. Among the four different supports applied, one can clearly distinguish two groups: catalysts with reducible supports ($ZrO_2$ and $TiO_2$) and catalysts with nonreducible supports ($\gamma$-$Al_2O_3$ and $SiO_2$). It is evident from Table 3 that the reducible supports displayed an appreciable decrease in the Pd/Me and Sb/Me ratios in the used samples compared with their corresponding fresh ones. This decrease in the surface ratios, particularly in the reducible supports, might be due to particle agglomeration and coke deposition. In particular, a preferred deposition of carbon on Pd cannot be excluded as a cause of the decreased Pd/Me ratios.

In contrast to reducible supports, the nonreducible supports ($Al_2O_3$, $SiO_2$) showed almost no considerable decrease in these

ratios and hence exhibited nearly constant surface Pd/Me and Sb/Me ratios in both the fresh and used samples. For better understanding, these results must be correlated with the TEM observations. On the first view, the changes of the Pd/Me ratios on $ZrO_2$-, $TiO_2$-, and $\gamma$-$Al_2O_3$-supported solids can be explained by the different agglomeration of the Pd nanoparticles on the different supports. This is not the case when $SiO_2$ is used as a support. Here a significant agglomeration can be observed by TEM that cannot be confirmed by the XPS results. Therefore, other factors (e.g., BET surface area) should influence the surface ratios. The differences in surface areas shown in Table 1 are reflected in the Pd/Me and Sb/Me ratios. Samples with a low BET surface area, like 10Pd8Sb/$ZrO_2$, are characterized by high values, whereas high-surface area samples like 10Pd8Sb/$SiO_2$ are characterized by low values. In this sample, the change in the amount of Pd atoms in the near-surface region during time on stream seems to be negligible compared with the high amount of Si atoms in this region, although agglomeration could be observed by TEM investigations. Next to this agglomeration, the influence of coke deposition and the formation of PdSb intermetallic phases on the Pd/Me surface ratio could not be excluded. On the whole, all of these different processes are expected to show considerable influence on the Pd/Me and Sb/Me ratios and complicate the explanation for the observed tendency of these ratios, which, however, undeniably depend on the nature of the support.

Interestingly, the tendency of changes in the surface ratios of Pd/Me and Sb/Me in the fresh and used solids is found to be more or less similar. In both cases, the reducible supports lose Pd and Sb to a certain extent in the near-surface region, whereas these changes are not so significant in the nonreducible supports. Such decreases in Pd/Me and Sb/Me (Me = Ti, Zr) ratios in the spent catalysts appear to be due mainly to coke deposits and represent a possible cause of catalyst deactivation. Unlike for Pd, no shift in the electron BE of Sb could be observed between the fresh and used samples. The BE of the Sb $3d_{3/2}$ electrons remained more or less constant at around 540 eV ($\pm$0.5 eV), corresponding to the valence states of +III or +V. Taking the preparation procedure into consideration, an oxidation state of +III seems more likely.

To gain new insight into and also to provide a first impression on the reactivity of the Pd particles, the amount of coke deposition on Pd in the near-surface region was estimated by XPS, and a factor involving the surface coke amounts was derived. For quantification, the factor developed by considering the ratios of C/Pd values between the used and fresh catalysts was correlated with the conversion of toluene; this is depicted in Fig. 5. It is noteworthy that the $TiO_2$-supported sample displayed the highest value of the factor (3.8), whereas the $\gamma$-$Al_2O_3$-supported one showed the lowest (1.9). The higher value of the factor observed for $TiO_2$ is unquestionably due to its higher activity compared with all other supports of this series. The difference in the value of this factor between the $ZrO_2$- and $Al_2O_3$-supported samples is not so significant, because the difference in the values of conversion levels of these two samples is also not very significant. In other words, both of these catalysts exhibited similar low toluene conversion levels

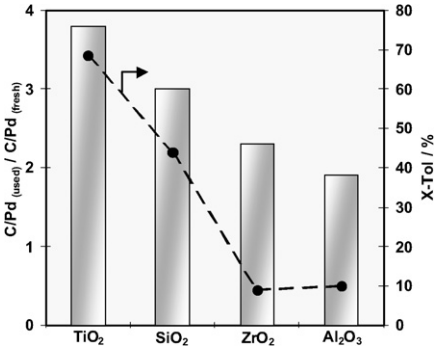


Fig. 5. Correlation of derived C/Pd factor with the catalytic activity of 10Pd8Sb catalysts with different supports.

($X$ = ca. 10%) and hence comparable values of the C/Pd factor around 2 (see Fig. 5). This factor derived from surface coke amounts is found to decrease in the following order:

$$TiO_2 > SiO_2 > ZrO_2 > \gamma\text{-}Al_2O_3. \quad \text{(ii)}$$

Interestingly, the above-described factor is observed to change more or less in a similar fashion as that of catalytic activity of the catalysts (as also shown below). It is reasonable to assume that high conversion of toluene causes increased deposition of coke. Therefore, one can presume that the catalysts with higher values of the factor will exhibit higher activity and vice versa. Hence, a good correlation between C/Pd factor and the catalytic activity can be established.

In addition to the issues discussed above, certain amounts of chloride species were observed on the surface of the samples, particularly the fresh samples. Detection of these surface chlorides by XPS in the fresh samples indicates that their concentration varied between 2 and 5 atom%. However, the chlorides were totally removed during the course of the reaction and under the influence of reactant feed mixture. Consequently, their concentration in the used samples can be estimated to be almost nil or only trace in some cases.

### 3.5. Pyridine adsorption and desorption

For characterizing the surface acidity, pyridine used as a probe molecule was adsorbed at room temperature. Generally, bands at around 1540–1548 and 1445–1460 $cm^{-1}$ are characteristic of Brønsted ($PyH^+$) and Lewis (L-Py) acid sites, respectively. Furthermore, bands of hydrogen-bonded pyridine (hb-Py) in the similar ranges of 1440–1447 and 1590–1600 $cm^{-1}$ and bands of physically adsorbed pyridine (ph-Py) at 1439 and 1580 $cm^{-1}$ are also expected [35–38]. Based on these assignments, in principle, discrimination between Lewis-bonded and hydrogen-bonded pyridine is not possible when the adsorption is carried out at ambient temperature. However, the thermal stability of the adsorbed pyridine species differs and increases in the following order: ph-Py < hb-Py < L-Py, $PyH^+$. Accordingly, Lewis-bonded pyridine needs to be properly determined by recording the infrared spectra at sufficiently high temperatures, to accomplish complete desorption of hb-Py.

The FTIR spectra obtained after adsorption of pyridine followed by evacuation of different supported PdSb solids and the

corresponding Pd materials are depicted in Fig. 6. The bands at around 1445 and 1540 $cm^{-1}$ characterize Lewis (LS) and Brønsted (BS) acidic sites, respectively. Our results show that all samples were dominated by Lewis acid sites, with only very low Brønsted acidity shown for the $Al_2O_3$- and $ZrO_2$-supported Sb solids.

The bands at around 1600 $cm^{-1}$ (see Fig. 6) are also due to pyridine adsorbed on Lewis sites and can be taken as a measure of the Lewis acid strength of the surface sites [38]. Whereas the bands at about 1595 $cm^{-1}$ arise from hydrogen-bonded pyridine or weak-medium Lewis sites, the bands at around 1605 $cm^{-1}$ are due to medium-strong Lewis sites.

It is interesting that the intensity of the band around 1595 $cm^{-1}$ is essentially lowered and in some cases totally disappeared in the PdSb catalysts compared with non-Pd-containing solids. In addition, a shift of the bands around 1444 $cm^{-1}$ to higher wavenumbers is observed. This result points to the fact that hydroxyl groups of the Sb-containing supports are involved in bonding with the Pd species.

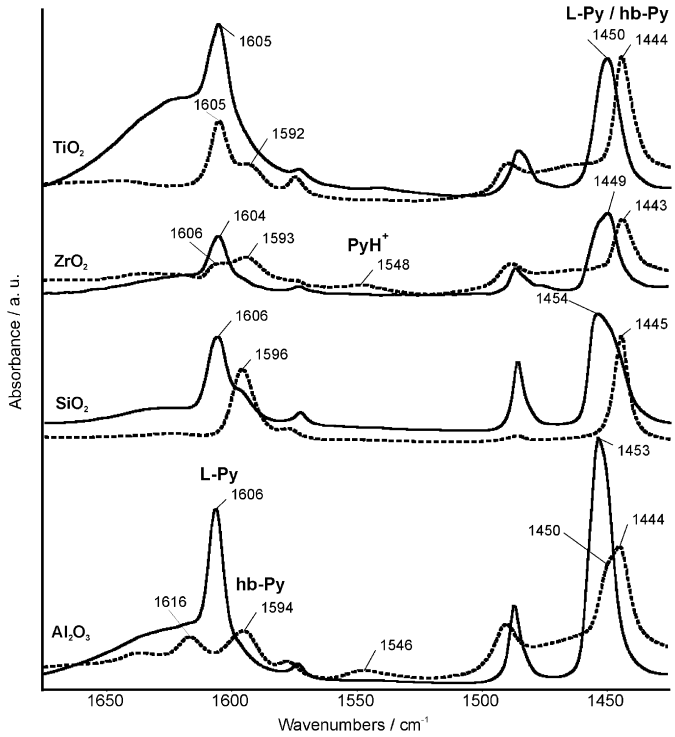


Fig. 6. FTIR spectra of pyridine adsorbed at room temperature on 8Sb (dotted lines) and 10Pd8Sb (solid lines) on different supports.

Comparing the spectra of supported Sb and PdSb solids, it is obvious that the appearance of strong new bands at around 1450 and 1604 $cm^{-1}$ indicates the creation of medium-strong Lewis acidic sites. The similar positions of these bands for all Pd samples point to the fact that the Lewis acidity is completely dominated by Pd species in the catalysts.

Table 4 presents BET surface areas and integral intensities of the bands at around 1450 $cm^{-1}$ (L-Py and hb-Py) of Sb and PdSb solids over different supports. The table clearly shows a dramatic increase in the Lewis acidity of the solids when palladium is added. This aspect is well evidenced by a clear jump of nearly two times in the values of integral intensities of each sample irrespective of support used. It should be noted that the band intensity is a measure of mainly hb-Py in the case of non-Pd-containing solids, whereas in the Pd-containing samples the band intensity represents only the amount of pyridine bonded to Lewis sites. If the integral intensities of the different samples are related to the specific surface areas, then comparable values are obtained for the $TiO_2$-, $ZrO_2$-, and $\gamma$-$Al_2O_3$-supported Pd catalysts, but an essentially lower value for the $SiO_2$-supported one. The lower value of the $SiO_2$-supported sample is due to the higher surface area of this solid compared with the others.

After evaluating such exciting observations on the effect of adding Pd on enhancing the Lewis acidity of the catalysts, further research was focused on the desorption behavior of adsorbed pyridine over a wide range of temperatures (25–350 °C). For this purpose, four solids (in the presence and absence of palladium) were selected, two from reducible supports ($8Sb/TiO_2$ and $10Pd8Sb/TiO_2$) and two from nonreducible supports ($8Sb/SiO_2$ and $10Pd8Sb/SiO_2$). The results are presented below.

The pyridine desorption spectra of $8Sb/TiO_2$ and $10Pd8Sb/TiO_2$ samples is are compared in Fig. 7. The band appearing at 1592 $cm^{-1}$ in the $8Sb/TiO_2$ solid can be attributed to hydrogen-bonded pyridine. However, this band disappeared at low temperature (100 °C), indicating the lower thermal stability of hb-Py. In addition to H-bonded pyridine, this $8Sb/TiO_2$ sample also exhibited two more intense bands at 1445 and 1605 $cm^{-1}$ that can be assigned to L-Py coordinatively bonded to $Ti^{4+}$ sites. The intensity of these two bands decreased gradually with increasing desorption temperature. Interestingly, these two bands were still observable even at 350 °C in the $8Sb/TiO_2$ solid, whereas they already vanished in $10Pd8Sb/TiO_2$ sample at this temperature. This fact suggests the existence of differ-

Table 4
BET surface areas and integral intensities of the bands around 1450 $cm^{-1}$ for supported Sb and PdSb catalysts

| Catalyst | $S_{BET}$ ($m^2/g$) | Integral intensity (a.u.) (absolute) | Integral intensity (a.u.) (related to $S_{BET}$) |
|---|---|---|---|
| $8Sb/TiO_2$ | 180.9 | 9.4 | 0.05 |
| $10Pd8Sb/TiO_2$ | 78.1 | 14.8 | 0.19 |
| $8Sb/ZrO_2$ | 138.0 | 3.4 | 0.02 |
| $10Pd8Sb/ZrO_2$ | 46.6 | 6.4 | 0.14 |
| $8Sb/SiO_2$ | 293.5 | 7.8 | 0.03 |
| $10Pd8Sb/SiO_2$ | 192.6 | 15.3 | 0.08 |
| $8Sb/\gamma$-$Al_2O_3$ | 188.2 | 8.4 | 0.04 |
| $10Pd8Sb/\gamma$-$Al_2O_3$ | 98.8 | 18.0 | 0.18 |

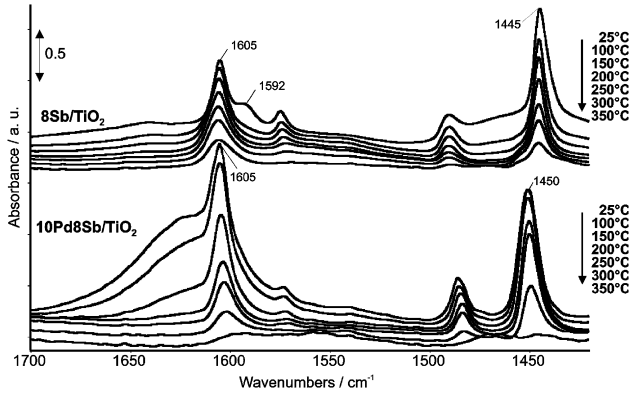


Fig. 7. Comparison of pyridine desorption spectra of $8Sb/TiO_2$ and $10Pd8Sb/TiO_2$ catalysts as a function of temperature.

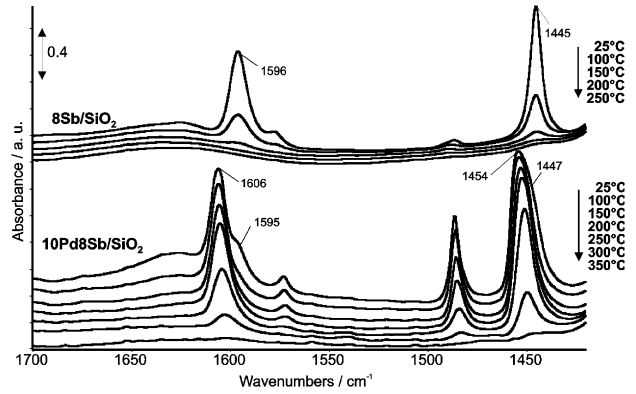


Fig. 8. Comparison of pyridine desorption spectra of $8Sb/SiO_2$ and $10Pd8Sb/SiO_2$ catalysts as a function of temperature.

ent kinds of Lewis sites with varying strengths in $8Sb/TiO_2$ and $PdSb/TiO_2$.

The desorption spectra of $8Sb/SiO_2$ and $10Pd8Sb/SiO_2$ are compared in Fig. 8. As observed earlier for $8Sb/TiO_2$, the band at 1596 $cm^{-1}$ also appeared in this $8Sb/SiO_2$ sample, which can be attributed to H-bonded pyridine interacting with surface Si–OH groups of the solid. This band disappeared during heating and completely vanished at 150 °C. Consequently, no Lewis acid sites exist in this sample. In contrast, the $10Pd8Sb/SiO_2$ sample exhibited two more bands at around 1450 and 1606 $cm^{-1}$, corresponding to Lewis acid sites resulting from $PdO_x$ species. The presence of these two bands even at higher temperatures in the pyridine desorption spectra indicates good thermal stability of these sites. Furthermore, the tendency of intensity changes of the Lewis band with increasing temperature is found to be more or less the same in both the$10Pd8Sb/SiO_2$ and $10Pd8Sb/TiO_2$ samples. This result points to the existence of equivalent $PdO_x$ species on both catalyst systems, which create the Lewis sites.

Taking into account the results shown in Figs. 7 and 8, clearly both the $10Pd8Sb/TiO_2$ and $10Pd8Sb/SiO_2$ samples contain a considerable amount of Lewis sites even at a desorption temperature of 250 °C, which is higher than the reaction temperature (210 °C) applied in the present study. Therefore, the presence of such higher amounts of Lewis sites at higher temperatures can be expected to significantly influence catalytic performance. On the other hand, one should also consider that very high acidity of the catalysts also may lead to higher coking and hence easy deactivation.

From the catalytic results, it is clear that the $10Pd8Sb/TiO_2$ sample displayed the best performance, followed by the $10Pd8Sb/SiO_2$ solid. However, if acidity alone is responsible for better performance, then the $\gamma$-$Al_2O_3$-supported 10Pd8Sb sample should have exhibited comparable performance; but this sample performed poorly despite its high Lewis acidity. This fact suggests that in addition to acidity, some other factor dominates the catalytic performance. Based on the catalytic results, this dominating factor appears to be Pd particle size. All of the investigations carried out so far show that the solids with larger Pd particles clearly have better performance and that the presence of Lewis sites further promotes catalytic performance. Therefore, it can be concluded that along with Pd particle size, Lewis acid sites also are responsible for the better catalytic activity of these samples.

### 3.6. Catalytic activity

#### 3.6.1. Influence of the support on the acetoxylation activity of toluene

All of the catalytic tests were carried out under optimized reaction conditions: molar ratio of toluene:acetic acid:oxygen (air):argon = 1:4:3(15):16, $T$ = 210 °C, GHSV (STP) = 2688 $h^{-1}$, and $\tau$ = 1.34 s. These conditions were established based on previous investigations [19]. Figs. 9a and 9b show the very recent and first results on the influence of support on the conversion of educts (toluene and acetic acid) and the product yields. It can be clearly seen that the nature of the support had a marked influence on the conversion of toluene as well as acetic acid; however, the selectivity of BA was almost independent of conversion and the nature of the support. The conversions of toluene and acetic acid varied from ca. 10 to 69% and from ca. 35 to 60%, respectively (Fig. 9a). The selectivity of BA changed over a small range, ca. 80–85% (within the margin of measurement error). Benzaldehyde (BAL) was the major byproduct of this reaction; the yields of BAL varied from 2 to 10% depending on the type of support used (Fig. 9b). $TiO_2$-supported PdSb catalyst exhibited superior performance, with high toluene conversion ($X$ = 68%) and high BA yield ($Y$ = ca. 58%). Both $ZrO_2$- and $Al_2O_3$-supported PdSb catalysts displayed the lowest performance ($X_{TOL}$ = ca. 10%; $S_{BA}$ = 81%). In addition, formation of greater amounts of $CO_x$ (up to 30%) was also observed over these two catalysts, undeniably due to the oxidative decomposition of acetic acid. Large differences in the conversion levels of toluene (ca. 10%) and acetic acid (ca. 35%) as well as from the yields of products such as BA ($Y$ = ca. 8%) and $CO_x$ (ca. 30%) provide further evidence that such oxidative decomposition of acetic acid was a predominant reaction over the $ZrO_2$- and $\gamma$-$Al_2O_3$ supported samples (Figs. 9a and 9b). Based on this result, it can be concluded that $ZrO_2$ and $\gamma$-$Al_2O_3$ are not suitable supports for this reaction, due mainly to unwanted enhancement in the oxidative decomposition of acetic acid rather than the desired improvement in the conversion of toluene with good selectivity toward BA. In

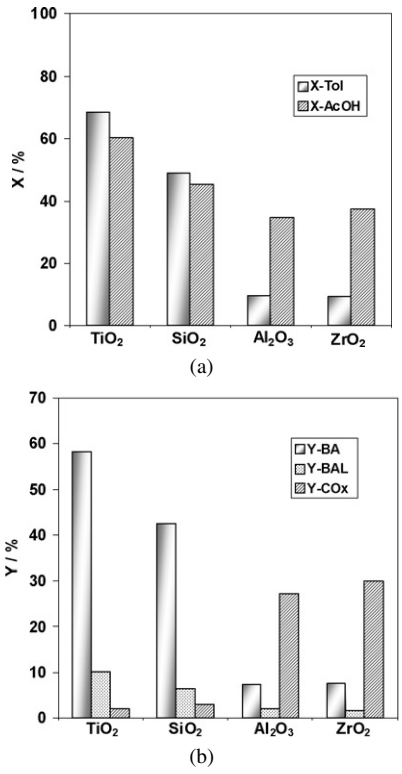


Fig. 9. (a) Influence of support on the conversion of educts over 10Pd8Sb/$MeO_x$ (MeO = $TiO_2$, $SiO_2$, $ZrO_2$, $\gamma$-$Al_2O_3$) catalysts (molar ratio of toluene: acetic acid:oxygen (air):argon = 1:4:3(15):16, $T$ = 210 °C, GHSV (STP) = 2688 $h^{-1}$, $\tau$ = 1.34 s; $X$-Tol = conversion of toluene, $X$-AcOH = conversion of acetic acid). (b) Comparison of the yields of products obtained over 10Pd8Sb/$MeO_x$ ($MeO_x$ = $TiO_2$, $SiO_2$, $ZrO_2$, $\gamma$-$Al_2O_3$) catalysts (molar ratio of toluene:acetic acid:oxygen (air):argon = 1:4:3(15):16, $T$ = 210 °C, GHSV (STP) = 2688 $h^{-1}$, $\tau$ = 1.34 s; $Y$-BA = yield of benzyl acetate, $Y$-BAL = yield of benzaldehyde, $Y$-$CO_x$ = yield of carbon oxides).

general, it has been observed that the catalysts containing larger Pd particles and having higher Lewis acidity displayed the better performance. Although the $\gamma$-$Al_2O_3$-supported solid had appreciably higher Lewis acidity, it contained mainly smaller Pd particles, whereas the $ZrO_2$-supported solid had very low Lewis acidity but a mixture of both smaller and (a few) larger Pd particles. In view of this finding, these two samples displayed poor performance. On the other hand, the $TiO_2$- and $SiO_2$-supported samples had higher acidity as well as larger Pd particles. Based on this criterion, the $TiO_2$- and $SiO_2$-supported solids exhibited much better performance than the other two samples.

It is important to note that the influence of reactant feed mixture is rather well manifested by a pronounced increase in the size of Pd particles during the course of reaction on almost all supports except $\gamma$-$Al_2O_3$. Such differences also can be assigned to different interactions between active Pd species and the support surface, particularly $\gamma$-$Al_2O_3$ with smaller Pd particles. These different interactions may further explain the variation in electronic properties of such less-reduced particles, which appears to be very sensitive to the chemical nature of their initial germination site on the oxide support. This result illustrates the possibility of differently dispersed Pd particles with different sizes and physicochemical properties.

Stakheev et al. [9] reported that Pd particles are electron-deficient on acidic supports and provide further possibilities for stabilization of small metal particles, for instance, by their accommodation as metal-proton adducts. In the present study, it has been observed that $\gamma$-$Al_2O_3$ displayed higher acidity than the other samples. Therefore, the acid sites on the surface of $\gamma$-$Al_2O_3$ may be considered to be surface centers stabilizing small metal particles and hence hindering the growth of Pd size during the course of the reaction, unlike other supports. Such stabilization of small metal particles is believed to be responsible for the poor performance of $\gamma$-$Al_2O_3$-supported solid. In addition, there is a general agreement that the support can stabilize certain types of surface faces with various structures and abilities to reconstruct. The support can also facilitate oxygen insertion into the subsurface layers of Pd, which generates strong distortions at the surface [39]. Comparing all of these effects clearly shows that the nature of support has a strong influence on catalytic performance and that the poor performance of $\gamma$-$Al_2O_3$-supported solid is incontestably due to the formation of smaller Pd particles in this sample.

### *3.6.2. Variation of conversion of educts and yields of products with time on stream over 10Pd8Sb solids with different supports*

Time-on-stream variation of conversions of educts and yields of products over 10Pd8Sb solids with different supports is displayed in Figs. 10a and 10b. One commonality among these catalysts is that all of the samples exhibited very low conversion of toluene (<5%), which increased considerably with time and then decreased again after a certain period (Fig. 10a). Such a substantial enhancement in toluene conversion with time on stream can be attributed to the formation of larger Pd particles during the course of the reaction, whereas the diminished catalytic activity with time is undoubtedly due to coke deposits. However, the deactivated catalysts can be easily regenerated in air (250 °C for 2 h) to restore the maximum activity that was lost due to coking. The regenerated catalysts immediately showed more or less similar performance as that of the maximally active catalyst due to burning of coke during regeneration in air. This aspect was well studied and clearly described in previous investigations [20]. Comparing the dependencies of Pd particle size and the catalytic activity clearly shows that the activity increased basically in the same manner as that of Pd particle size. Apparently, Pd surface atoms on larger particles are more active than those on smaller ones. This corroborates the assumption that the reaction occurs more effectively on larger Pd surface sites, which seem to be highly defective. The tendency also agrees well with previous findings [20–22] and reconfirms the dominant influence of Pd particle size on catalytic performance.

Although the tendency toward increased toluene conversion and BA yield (Figs. 10a and 10b) were found to be more or less similar in all of the catalysts, certain differences remained, particularly in the level of performance. As described above, the $TiO_2$-supported solid displayed the best performance in view of its high Lewis acidity and larger Pd particles, whereas the $\gamma$-$Al_2O_3$- and $ZrO_2$-supported solids gave poor performance

due to the presence of smaller Pd particles in them. On the other hand, the maximum conversion of acetic acid (>35%) obtained over these two catalysts ($\gamma$-$Al_2O_3$- and $ZrO_2$-supported ones) was nearly four times higher than the conversion of toluene (9%) (Fig. 10a). Similarly, the yield of $CO_x$ (⩾30%) was also four times higher than the yield of BA (ca. 8%) (Fig. 10b). This result clearly suggests that $CO_x$ formation occurs mainly from the decomposition of acetic acid, not from toluene. Similar observations were also found in earlier investigations [20].

The conversion of toluene over 10Pd8Sb/$TiO_2$ solid increased from 35% after the first hour to a maximum of 68.5% after ca. 12 h and then decreased to 30% after 34 h on stream (Fig. 10a). The variation in BA yield with time on stream was found to change in exactly the same manner as that of conversion; this is because the selectivity of BA is independent of conversion of toluene. A similar tendency was also seen for the other catalysts, with the only difference being in the time (ca. 3 h) needed to attaining steady-state conditions. These differences in the time needed to achieve steady-state conditions in these catalysts can be expected from the differences in the size of Pd particles associated with them. It is quite reasonable to assume that the growth of Pd to 100 nm takes more time than the growth to only 10 nm; thus, it is not surprising that the $TiO_2$-supported sample with the largest Pd particles (ca. 100 nm) took longer than the others. Furthermore, the growth mechanism of Pd particles also might be different and may depend on the nature of the support applied. As expected, the $\gamma$-$Al_2O_3$- and $ZrO_2$-supported solids took only 3 h because of their small Pd particles (ca. 10 nm), but surprisingly even the $SiO_2$-supported solid took a similar amount of time, even though it contained some larger Pd particles (up to 60 nm). This result indicates that Pd growth in $SiO_2$-supported catalyst is either faster or occurs through a different mechanism.

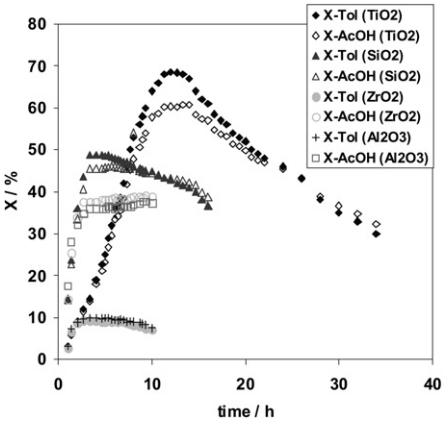


(a)

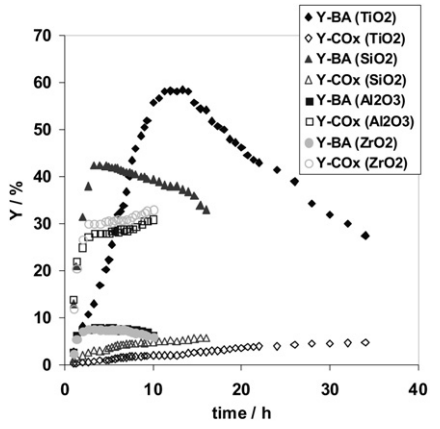


(b)

Fig. 10. (a) Variation of conversion of educts with time-on-stream over 10Pd-8Sb solids with different supports (molar ratio of toluene:acetic acid: oxygen (air):argon = 1:4:3(15):16, $T$ = 210 °C, GHSV (STP) = 2688 $h^{-1}$, $\tau$ = 1.34 s; $X$-Tol = conversion of toluene, $X$-AcOH = conversion of acetic acid). (b) Variation of yields of products with time-on-stream over 10Pd8Sb solids with different supports (molar ratio of toluene:acetic acid:oxygen (air):argon = 1:4:3(15):16, $T$ = 210 °C, GHSV (STP) = 2688 $h^{-1}$, $\tau$ = 1.34 s; $Y$-BA = yield of benzyl acetate, $Y$-$CO_x$ = yield of carbon oxides).

Normally, one would expect higher activity from small Pd particles due to their high dispersion and efficient adsorption. However, our findings show that the larger Pd particles were always much more active than the smaller ones. Although this phenomenon is somewhat unusual, some studies have found larger Pd particles to be more active than smaller ones, particularly in the hydrogenation of alkynes (e.g., 1-butyne) [40] or vinyl acetate [41]. Those authors interpreted their results in terms of the adsorption strength of reactant molecules. Similar reports on the increased catalytic activity with increasing Pd particle size have been published previously [42–44]. The decreased catalytic activity with decreasing Pd particle size was also explained by the changes in the electronic structure of small Pd nanoparticles, leading to stronger interaction with the educt (e.g., 1,3-butadiene) and easy deactivation. Similar modifications also can be expected in the catalysts that we studied. Based on these results, more pronounced differences in the catalytic behavior of very small and large Pd particles have been found.

Table 5
Comparison of coke deposits in the used catalysts and duration of the tests over 10Pd8Sb samples with different supports

| Catalyst | Coke (%) | Time-on-stream (h) |
|---|---|---|
| 10Pd8Sb/$TiO_2$ | 6.3 | 34 |
| 10Pd8Sb/$ZrO_2$ | 4.3 | 10 |
| 10Pd8Sb/$SiO_2$ | 5.8 | 16 |
| 10Pd8Sb/$\gamma$-$Al_2O_3$ | 4.7 | 10 |

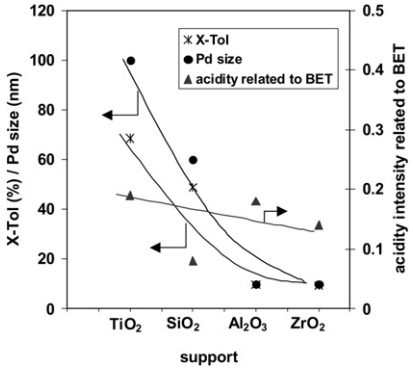


Fig. 11. Correlation of Pd particle size and Lewis acid strength with the catalytic activity of 10Pd8Sb catalysts over different supports.

The duration of the catalytic tests and the amount of coke deposits estimated in the spent PdSb catalysts with different supports is presented in Table 5. Among all of the catalysts, the $TiO_2$-supported catalyst was tested for a longer time (34 h) in view of its better performance. However, the estimated coke content was comparable (5–6%) in all of these catalysts but marginally higher in the $TiO_2$-supported one, probably due to the longer duration of the tests as well as the higher conversion levels of educts.

### *3.7. Correlation of Pd particle size and Lewis acid strength with the catalytic activity of 10Pd8Sb catalysts over different supports*

An attempt was made in the present investigation to derive acidity–activity relationships for the present acetoxylation of toluene. Fig. 11 demonstrates the correlation of Pd particle size and Lewis acidity with the catalytic activity of PdSb solids with different supports. The catalytic activity is seen to change in a similar way as the Pd particle size and Lewis acidity of the catalysts. Interestingly, a very close correlation between Pd particle size and conversion of toluene can be seen (see Fig. 11). It appears that the metal particle growth or redispersion brought about by reaction conditions seems to enhance the catalytic activity of the catalysts. The results presented in Fig. 11 provide good evidence that the catalytic activity is indisputably dependent on the Pd particle size and the Lewis acidity of the catalysts.

Despite the higher acidity of the $\gamma$-$Al_2O_3$-supported catalyst, this catalyst's catalytic performance was much inferior to that of the $TiO_2$-supported catalyst. Consequently, we can infer that Pd particle size is highly dominant over the acidity characteristics of the solids, and thus it becomes easy to distinguish the distinct influence of Pd particle size on catalytic performance. Among all of the supports studied, the $TiO_2$-supported catalyst contained the majority of larger Pd particles (100 nm) and had relatively higher acidity and thus the highest activity. $SiO_2$ displayed the next-best performance. However, $SiO_2$ as an inert support did not influence the activity of Pd to the same extent as the acidic and reducible $TiO_2$ with larger Pd particles.

The decreasing order of activity and Pd size was as follows:

$$TiO_2 > SiO_2 > ZrO_2 \sim \gamma\text{-}Al_2O_3. \quad \text{(iii)}$$

The decreasing order of Lewis of acidity related to BET surface area occurred in the following order:

$$TiO_2 \sim \gamma\text{-}Al_2O_3 > ZrO_2 > SiO_2. \quad \text{(iv)}$$

Comparing these two tendencies shows that Lewis acidity appears to be the next important factor after Pd particle size. This result also provides further evidence that any highly active and selective toluene acetoxylation catalyst should contain larger Pd particles and highly pronounced Lewis acidity. Another aspect of the evaluation of Pd catalysts during the reaction is the change in the electronic properties of palladium species. We also observed the superactivity of larger Pd particles in previous investigations [14,17,18]. It is thus possible to establish a correlation between the size of Pd particles and the activity of the catalysts. Based on these investigations, a good consensus can be reached that Pd particle size is the crucial and dominant parameter among the factors responsible for improving catalyst performance.

## 4. Conclusions

The nature of the support has a significant influence on Pd particle size, valence states, and acidity characteristics of catalysts. The prominent catalytic properties exhibited by the catalysts studied herein can be ascribed mainly to the formation of larger Pd particles during the course of the reaction. TEM clearly showed a remarkable growth in the size of Pd particles in the used samples compared with the corresponding fresh samples. However, the increase in Pd size was found to be dependent on the nature of the support. The growth of Pd particles during the course of the reaction was proven to be indispensable for improving catalytic performance. The phase composition of the solids at the surface (XPS) was found to be somewhat different from that in the bulk (XRD). XPS showed a significant influence of the support on the reducibility of the palladium species. Interestingly, a good correlation between the factor derived from surface C/Pd ratios and the catalytic activity was established. The application of FTIR spectroscopy using pyridine as probe molecule proved useful for direct monitoring of interactions between adsorbed molecules and catalyst. Acidity measurements also revealed an appreciable influence of the type of support on the nature and strength of acid sites. Lewis acidity was completely dominated in all PdSb catalysts and was found to be an important factor in improving catalytic performance. Among the various supports tested, titania (anatase) displayed the best performance, whereas zirconia and $\gamma$-$Al_2O_3$ exhibited poor performance for similar Pd and Sb loadings.

Next to the size of Pd particles, Lewis acidity appears to be the most important factor in enhancing catalytic performance. Thus, it can be concluded that suitably tailoring Pd particle size and acidity characteristics is essential to improving the catalytic properties of the catalysts. Finally, these innovative results are expected to provide new opportunities for investigations into the structure–activity relationships in supported metal catalysts and thus may help gradually expand the scope of these investigations in developing novel catalyst compositions that can be effectively used for various other industrially important acetoxylation reactions. Further studies will presumably shed more light on these topics.

## Acknowledgments

The authors are thankful to Dr. M. Schneider, Mrs. S. Evert, Mrs. U. Wolf, and Mrs. W. Winkler for their help in characterizing the samples by various techniques.

## References

[1] P. Panagiotopoulou, D.I. Kondarides, Catal. Today 112 (2006) 49.
[2] K. Persson, A. Ersson, S. Colussi, A. Trovarelli, S.G. Jaras, Appl. Catal. B 66 (2006) 175.

[3] M. Schmal, M.M.V.M. Souza, V.V. Alegre, M.A. Pereira da Silva, D.V. César, C.A.C. Perez, Catal. Today 118 (2006) 392.
[4] B. Imelik (Ed.), Metal-Support and Metal-Additive Effects in Catalysis, Elsevier, Amsterdam, 1982.
[5] G.C. Bond, R. Burch, Specialist Periodical Reports: Catalysis, vol. 6, Royal Society of Chemistry, London, 1983, p. 27.
[6] R. Burch, Specialist Periodical Reports: Catalysis, vol. 7, Royal Society of Chemistry, London, 1995, p. 149.
[7] R.L. Moss, Specialist Periodical Reports: Catalysis, vol. 4, Royal Society of Chemistry, London, 1981, p. 31.
[8] T. Ishihara, K. Harada, K. Eguchi, H. Arai, J. Catal. 136 (1992) 161.
[9] A.Y. Stakheev, L.M. Kustov, Appl. Catal. A 188 (1999) 3.
[10] C.H. Bartholomew, R.B. Pannell, J.L. Butler, J. Catal. 65 (1980) 335.
[11] D.A. Hickman, L.D. Schmidt, J. Catal. 138 (1992) 267.
[12] S.S. Bharadwaj, L.D. Schmidt, Fuel Process Technol. 42 (1995) 109.
[13] M. Lyubovsky, L. Pfefferle, Catal. Today 47 (1999) 29.
[14] A. Benhmid, K.V. Narayana, A. Martin, B. Lücke, Chem. Commun. (2004) 2118.
[15] L. Eberson, L. Jönsson, Acta Chem. Scand. B 28 (1974) 597.
[16] T. Komatsu, K. Inaba, T. Uezono, A. Onda, T. Yashima, Appl. Catal. A 251 (2003) 315.
[17] A. Benhmid, K.V. Narayana, A. Martin, B. Lücke, M.-M. Pohl, Chem. Lett. 33 (2004) 1238.
[18] A. Benhmid, K.V. Narayana, A. Martin, B. Lücke, M.-M. Pohl, Chem. Commun. (2004) 2416.
[19] A. Benhmid, K.V. Narayana, A. Martin, B. Lücke, M.-M. Pohl, Catal. Today 112 (2006) 192.
[20] A. Benhmid, K.V. Narayana, A. Martin, B. Lücke, S. Bischoff, M.-M. Pohl, J. Radnik, M. Schneider, J. Catal. 230 (2005) 420.
[21] V.N. Kalevaru, A. Benhmid, J. Radnik, B. Lücke, A. Martin, J. Catal. 243 (2006) 25.
[22] J. Radnik, A. Benhmid, K.V. Narayana, A. Martin, B. Lücke, M.-M. Pohl, U. Dingerdissen, Angew. Chem. Int. Ed. 44 (2005) 6771.
[23] J. Ryczkowski, Catal. Today 68 (2001) 263.
[24] J.A. Rabo, G.J. Gajda, Catal. Rev. Sci. Eng. 31 (1989/1990) 385.
[25] G. Marcelin, in: J.J. Spivey, S.K. Agarwal (Eds.), Catalysis, vol. 10, Royal Society of Chemistry, Cambridge, 1993, p. 83.
[26] W.E. Parneth, R.J. Gorte, Chem. Rev. 95 (1995) 615.
[27] A. Benhmid, K.V. Narayana, A. Martin, B. Lücke, S. Bischoff, DE 10 2004 002 262 A1 (2005).
[28] A. Benhmid, A. Martin, K.V. Narayana, B. Lücke, S. Bischoff, WO 2005/066107 A1 (2005).
[29] W. Juszezyk, A. Malinowski, Z. Karpinski, Appl. Catal. A 166 (1998) 311.
[30] N. Krishnankutty, M.A. Vannice, J. Catal. 155 (1995) 312.
[31] N. Krishnankutty, J. Li, M.A. Vannice, Appl. Catal. A 173 (1998) 137.
[32] W.-J. Shen, M. Okumura, Y. Matsumura, M. Haruta, Appl. Catal. A 213 (2001) 225.
[33] D.I. Kochubey, S.N. Pavlova, B.N. Novgorodov, G.N. Krykukova, V.A. Sadykov, J. Catal. 161 (1996) 500.
[34] M. Lyubovsky, L. Pfefferle, A. Datye, J. Bravo, T. Nelson, J. Catal. 187 (1999) 275.
[35] E.P. Parry, J. Catal. 2 (1963) 371.
[36] R. Buzzoni, S. Bordiga, G. Ricchiardi, C. Lamberti, A. Zecchina, G. Bellussi, Langmuir 12 (1996) 930.
[37] G. Busca, Catal. Today 41 (1998) 191.
[38] G. Busca, Phys. Chem. Chem. Phys. 1 (1999) 723.
[39] S.N. Pavlova, V.A. Sadykov, V.A. Razdobarov, E.A. Paukshtis, J. Catal. 161 (1996) 507.
[40] S. Hub, L. Hilaire, R. Touroude, Appl. Catal. 36 (1988) 307.
[41] Y.A. Ryndin, L.V. Nosova, A.L. Boronin, A.L. Chuvilin, Appl. Catal. 42 (1988) 131.
[42] J.P. Boitiaux, J. Cosyns, S. Vasudevan, Appl. Catal. 6 (1983) 41.
[43] B. Tardy, C. Noupa, C. Leclercq, J.C. Bertolini, A. Hoareau, M. Treilleux, J.P. Faure, G. Nihoul, J. Catal. 129 (1991) 1.
[44] J.C. Bertolini, P. Delichere, B. Khanra, J. Massardier, C. Noupa, B. Tardy, Catal. Lett. 6 (1990) 215.